

2010-01-01

## Enhancement of the Antibacterial Properties of Silver Nanoparticles Using Beta-Cyclodextrin as a Capping Agent

Swarna Jaiswal

Technological University Dublin, swarna.jaiswal@tudublin.ie

Brendan Duffy

Technological University Dublin, brendan.duffy@tudublin.ie

Niall Stobie

Technological University Dublin, niall.stobie@tudublin.ie

See next page for additional authors

Follow this and additional works at: <https://arrow.tudublin.ie/cenresart>

 Part of the [Pathogenic Microbiology Commons](#)

---

### Recommended Citation

Jaiswal, S., Duffy, B., Kumar, A., Stobie, N., McHale, P.: Enhancement of the antibacterial properties of silver nanoparticles using b-cyclodextrin as a capping agent. *International Journal of Antimicrobial Agents* Volume 36, Issue 3, September 2010, Pages 280-283. doi:10.1016/j.ijantimicag.2010.05.006

This Article is brought to you for free and open access by the Crest: Centre for Research in Engineering Surface Technology at ARROW@TU Dublin. It has been accepted for inclusion in Articles by an authorized administrator of ARROW@TU Dublin. For more information, please contact [arrow.admin@tudublin.ie](mailto:arrow.admin@tudublin.ie), [aisling.coyne@tudublin.ie](mailto:aisling.coyne@tudublin.ie).



This work is licensed under a [Creative Commons Attribution-NonCommercial-Share Alike 4.0 License](#)  
Funder: DIT ABBEST

---

**Authors**

Swarna Jaiswal, Brendan Duffy, Niall Stobie, Patrick McHale, and Amit Jaiswal



Contents lists available at ScienceDirect

## International Journal of Antimicrobial Agents

journal homepage: <http://www.elsevier.com/locate/ijantimicag>



Short communication

# Enhancement of the antibacterial properties of silver nanoparticles using $\beta$ -cyclodextrin as a capping agent

Swarna Jaiswal<sup>a,b</sup>, Brendan Duffy<sup>b,\*</sup>, Amit Kumar Jaiswal<sup>c</sup>, Niall Stobie<sup>b</sup>, Patrick McHale<sup>a</sup>

<sup>a</sup> School of Biological Sciences, Dublin Institute of Technology, Kevin Street, Dublin 8, Ireland

<sup>b</sup> Centre for Research in Engineering Surface Technology (CREST), FOCAS Institute, Dublin Institute of Technology, Dublin 8, Ireland

<sup>c</sup> School of Food Science and Environmental Health, Dublin Institute of Technology, Cathal Brugha Street, Dublin 1, Ireland

### ARTICLE INFO

#### Article history:

Received 16 November 2009

Accepted 19 May 2010

#### Keywords:

$\beta$ -Cyclodextrin

Silver nanoparticles

Antibacterial activity

### ABSTRACT

Silver nanoparticles (AgNPs) were synthesised by reducing silver salts using NaBH<sub>4</sub> followed by capping with varying concentrations of  $\beta$ -cyclodextrin ( $\beta$ -CD) and were physically characterised. Antibacterial activity against *Escherichia coli*, *Pseudomonas aeruginosa* and *Staphylococcus aureus* was determined by a microtitre well method. The AgNPs were spherical under transmission electron microscopy, whilst dynamic light scattering showed average diameters of capped particles to be smaller (4–7 nm) than their uncapped equivalents (17 nm). Capped particles demonstrated superior photostability when exposed to intense ultraviolet radiation for 4 h as well as significantly ( $P < 0.05$ ) higher (up to 3.5-fold) antibacterial activity. The influence of  $\beta$ -CD concentration was seen to delay bacterial growth, indicating that a Trojan horse mechanism may be occurring owing to bacterial carbohydrate affinity, thereby enhancing silver ion absorption.

© 2010 Elsevier B.V. and the International Society of Chemotherapy. All rights reserved.

## 1. Introduction

The persistence of antibiotic-resistant bacteria has renewed interest in the use of silver and silver-based compounds, including silver nanoparticles (AgNPs), as alternative antibacterial agents. Such compounds can reduce infections in burns patients and prevent bacterial colonisation of prostheses, catheters, dental materials and human skin. The high thermal stability, low toxicity to human cells and effective broad-spectrum antibacterial activity of AgNPs [1] have been exploited in a range of commercial products.

There are several hypotheses to explain the antibacterial activity of AgNPs. Their rapid breakdown releases ionic silver that inactivates vital bacterial enzymes by interacting with essential thiol groups. Silver ions can inhibit bacterial DNA replication, damaging bacterial cytoplasmic membranes, depleting levels of intracellular adenosine triphosphate (ATP) and causing cell death [2]. The high specific surface-to-volume ratio of AgNPs increases their contact with microorganisms, promoting the dissolution of silver ions, thereby improving biocidal effectiveness. The ability of AgNPs to release silver ions is key to their antibacterial activity [3].

AgNPs can be synthesised in a number of ways, with borohydride reduction of silver salts being the most common. Stabilisation is achieved using capping agents that bind to the nanoparticle surface and improve stability and water solubility,

which are essential to prevent aggregation; examples include water-soluble polymers, oligosaccharides and polysaccharides, sodium dodecyl sulphate (SDS) and sophorolipid (glycolipid) [4].

Cyclodextrins (CDs) are a family of soluble, non-toxic molecules consisting of 6, 7 or 8 D-glucopyranosyl residues (denoted as  $\alpha$ -,  $\beta$ - and  $\gamma$ -CDs, respectively) linked in cyclic structure by  $\alpha$ -1,4 glycosidic bonds. They can form inclusion complexes incorporating various molecular guests within their hollow, truncated cone-shaped cavity structure, enabling them to be used as drug carriers and enzyme mimics. Host–guest interaction has been attributed to a combination of weak interactions such as van der Waals forces, hydrogen bonding and hydrophobic interactions [5]. Of the three cyclodextrins,  $\beta$ -CD, with an internal cavity diameter of 0.78 nm, is the most widely used but is too small to entrap AgNPs and simply binds via chemisorption to the nanoparticles through rim hydroxyl groups.

Unmodified  $\beta$ -CD has been used to prepare silver and gold nanoparticles in the presence of different reducing agents such as ethanol, dimethylformamide, ethylene glycol and sodium citrate. Little has been published on the antimicrobial activity of unmodified CDs, but modified  $\beta$ -CD (dimethylated  $\beta$ -CD) inhibited growth of *Rhodococcus erythropolis* and hydroxypropyl- $\beta$ -CD was toxic for *Mycoplasma capricolum* and *Acholeplasma laidlawii*, whilst methylated  $\beta$ -CD altered growth and cell envelope features of *Mycobacterium* sp. [6].

The present work investigated AgNP synthesis using different concentrations of unmodified  $\beta$ -CD with NaBH<sub>4</sub> as the

\* Corresponding author. Tel.: +353 1 402 7964.

E-mail address: [brendan.duffy@dit.ie](mailto:brendan.duffy@dit.ie) (B. Duffy).

reducing agent. AgNPs were characterised by ultraviolet–visible (UV–Vis) spectrometry, Fourier transform infrared spectroscopy (FT-IR), dynamic light scattering (DLS) and transmission electron microscopy (TEM). Antibacterial activities of uncapped and  $\beta$ -CD-capped AgNPs against Gram-negative (*Escherichia coli* and *Pseudomonas aeruginosa*) and Gram-positive (*Staphylococcus aureus*) bacteria were determined.

## 2. Materials and methods

### 2.1. Synthesis of silver nanoparticles

Aqueous  $\beta$ -CD solutions (5, 10 and 20 mM) were stirred into equal volumes of 2 mM AgNO<sub>3</sub> for 15 min and equal volumes of ice-cold 20 mM NaBH<sub>4</sub> were added. Resultant solutions were stabilised by stirring (24 h). The final molar ratios of  $\beta$ -CD:AgNO<sub>3</sub> were 2.5, 5 and 10 to 1, respectively. A  $\beta$ -CD-free control was similarly prepared. All chemicals were purchased from Sigma-Aldrich (Dublin, Ireland) and were used without further purification.

### 2.2. Sample characterisation

UV–Vis absorption spectra of  $\beta$ -CD-capped AgNPs were acquired in the 300–800 nm wavelength range using an UV–Vis–NIR spectrophotometer (Perkin-Elmer Lambda 900; Perkin-Elmer) operating at a resolution of 2 nm. FT-IR spectra were measured in the 4000–400 cm<sup>-1</sup> range with a resolution of 1 cm<sup>-1</sup> using a Perkin-Elmer Spectrum GX instrument in transmission mode using potassium bromide (KBr) pellets prepared by mixing KBr powder with AgNP solutions and then drying (24 h, 100 °C). AgNP morphology was determined using a JEM-100CX II transmission electron microscope (JEOL) operated at an accelerating voltage of 100 kV. Samples were drop-cast onto standard Formvar-coated copper grids (200–300 nm) and then air dried. The average particle size (hydrodynamic diameter) was determined at 25 °C by DLS using a Malvern Zetasizer Nano instrument (Malvern Instruments) equipped with a 4 mW He–Ne laser and measured using an automatic mode with a scattering angle of 90°. Sample photostability was determined by exposing solutions to an intense UV source (Q-sun Xenon Test Chamber; Q-Lab) operating at 0.4 W/m<sup>2</sup> (340 nm) for 1, 2, 3 and 4 h, respectively.

### 2.3. Bacterial strains and growth conditions

Gram-negative bacteria (*E. coli* ATCC 11229 and *P. aeruginosa* ATCC 27852) and Gram-positive bacteria (*S. aureus* ATCC 25923) were grown, subcultured and maintained on Mueller–Hinton agar (Lab M) and stored at 4 °C. For the experiment, a single colony of each organism was inoculated into 10 mL of Mueller–Hinton broth (MHB) and incubated overnight at 37 °C with shaking at 200 rpm. The optical density of the overnight culture was adjusted to that of a 0.5 McFarland standard [ $1.5 \times 10^8$  colony-forming units (CFU)/mL] using a Densimat photometer (bioMérieux, France) and diluted with MHB to give a final working concentration of  $1 \times 10^6$  CFU/mL.

### 2.4. Antibacterial activity assay

Antibacterial activities of capped and uncapped AgNPs of different silver concentrations were determined by a microtitre well method [7]. Samples were doubly diluted in water (100  $\mu$ L) in microtitre wells and bacteria (100  $\mu$ L;  $10^6$  CFU/mL) were added. Negative (AgNPs 100  $\mu$ L + sterile MHB 100  $\mu$ L) and positive (sterile MHB 100  $\mu$ L + bacterial suspension 100  $\mu$ L) control wells and a sterility control blank (sterile MHB 200  $\mu$ L) were included in each assay. Plates were incubated (18 h) in a microtitre plate reader (PowerWave™ Microplate spectrophotometer; BioTek, Winooski,

VT) at 37 °C. Samples were tested in duplicate on each plate and each plate was analysed in triplicate.

### 2.5. Data analysis

#### 2.5.1. Percentage inhibition of growth

AgNP antibacterial activities were determined by calculating the percentage inhibition of growth using the formula [7]:

$$I\% = \frac{(C_{18} - C_0) - (T_{18} - T_0)}{(C_{18} - C_0)} 100$$

where  $I$  is the percentage inhibition of growth,  $C_{18}$  is the blank-compensated optical density at 600 nm ( $OD_{600}$ ) of the positive control of the organism at 18 h,  $C_0$  is the blank-compensated  $OD_{600}$  of the positive control of the organism at 0 h,  $T_{18}$  is the negative control-compensated  $OD_{600}$  of the organism in the presence of test sample at 18 h, and  $T_0$  is the negative control-compensated  $OD_{600}$  of the organism in the presence of test sample at 0 h.

#### 2.5.2. Kinetic measurement of bacterial growth

Bacterial concentrations in the presence of capped and uncapped AgNPs were determined over time by measuring the  $OD_{600}$  every 30 min following 30 s of agitation. Antibacterial kinetics was analysed graphically as a plot of contact time versus  $OD_{600}$ .

#### 2.5.3. Statistical analysis

Statistical differences between multiple comparisons were evaluated using analysis of variance (ANOVA) followed by least significant difference testing. All statistical analyses were carried out using STATGRAPHICS centurion XV. A  $P$ -value of  $<0.05$  was considered statistically significant.

## 3. Results and discussion

### 3.1. Characterisation of $\beta$ -cyclodextrin-capped silver nanoparticles

All AgNPs showed a surface plasmon absorption band around 400 nm as expected for colloidal AgNPs, indicating roughly spherical nanoparticles, whilst solution absorbance intensities increased with  $\beta$ -CD concentration. Since the intensity of the plasmon resonance band depends on particle size, shape, metallic material and its surrounding environment, the number of particles cannot be related linearly to the absorbance intensities [8].

### 3.2. Ultraviolet stability

On exposure to intense UV radiation the colour of uncapped AgNPs became darker, with the absorbance peak becoming 14.05 nm broader (with respect to peak width at half maximum) over time. There were no significant changes in absorbance at the higher  $\beta$ -CD concentrations, although at 5 mM it increased slightly. This confirmed that uncapped AgNPs continued to grow and/or aggregate over time, whilst AgNPs capped at appropriate  $\beta$ -CD concentrations exhibited good stability.

### 3.3. Silver nanoparticle– $\beta$ -cyclodextrin binding

FT-IR confirmed  $\beta$ -CD binding to the AgNP surface. The free  $\beta$ -CD spectrum showed bands at 947 cm<sup>-1</sup> (skeletal vibration involving  $\alpha$  1–4 linkage) and 756 cm<sup>-1</sup> (ring breathing vibration), whilst bands at 708 cm<sup>-1</sup> and 579 cm<sup>-1</sup> were assigned to pyranose ring vibration [9]. Comparison of the spectra of 20 mM  $\beta$ -CD-capped AgNPs and free  $\beta$ -CD showed a decrease in the relative intensities of transmittance bands at 947 cm<sup>-1</sup>, 756 cm<sup>-1</sup>, 708 cm<sup>-1</sup> and 579 cm<sup>-1</sup> and a suppression of the –OH vibrational band at

**Table 1**

Percentage growth inhibition of *Pseudomonas aeruginosa*, *Escherichia coli* and *Staphylococcus aureus* in the presence of uncapped and  $\beta$ -cyclodextrin ( $\beta$ -CD)-capped (5, 10 and 20 mM) silver nanoparticles (AgNPs) containing different silver concentrations<sup>a</sup>.

Microorganism	Sample	[Ag]					
		100 ppm	50 ppm	25 ppm	12.5 ppm	6.25 ppm	3.12 ppm
<i>P. aeruginosa</i>	20 mM $\beta$ -CD–AgNPs	99.72 $\pm$ 0.2	96.11 $\pm$ 3.7	98.36 $\pm$ 1.1	99.24 $\pm$ 0.5	N/D	N/D
<i>P. aeruginosa</i>	10 mM $\beta$ -CD–AgNPs	99.08 $\pm$ 0.8	98.59 $\pm$ 1.5	98.34 $\pm$ 1.4	97.27 $\pm$ 0.7	N/D	N/D
<i>P. aeruginosa</i>	5 mM $\beta$ -CD–AgNPs	99.85 $\pm$ 0.4	97.23 $\pm$ 1.5	98.37 $\pm$ 1.1	64.50 $\pm$ 6.2	N/D	N/D
<i>P. aeruginosa</i>	Uncapped AgNPs	97.40 $\pm$ 2.2	96.55 $\pm$ 1.3	96.23 $\pm$ 3.1	13.92 $\pm$ 6.6	N/D	N/D
<i>E. coli</i>	20 mM $\beta$ -CD–AgNPs	99.19 $\pm$ 0.3	96.81 $\pm$ 2.9	96.91 $\pm$ 1.6	98.40 $\pm$ 0.7	53.45 $\pm$ 4.8	34.84 $\pm$ 5.8
<i>E. coli</i>	10 mM $\beta$ -CD–AgNPs	100 $\pm$ 0	96.96 $\pm$ 2.9	97.01 $\pm$ 1.4	97.02 $\pm$ 0.6	43.66 $\pm$ 3.3	20.09 $\pm$ 4.6
<i>E. coli</i>	5 mM $\beta$ -CD–AgNPs	99.59 $\pm$ 0.4	97.38 $\pm$ 3.3	97.91 $\pm$ 2.0	97.39 $\pm$ 0.2	29.28 $\pm$ 10.9	19.38 $\pm$ 3.2
<i>E. coli</i>	Uncapped AgNPs	100 $\pm$ 0	96.52 $\pm$ 2.4	97.73 $\pm$ 0.7	97.58 $\pm$ 2.3	22.75 $\pm$ 10.3	17.3 $\pm$ 1.0
<i>S. aureus</i>	20 mM $\beta$ -CD–AgNPs	99.76 $\pm$ 0.3	97.75 $\pm$ 2.6	96.99 $\pm$ 1.2	97.48 $\pm$ 0.8	97.14 $\pm$ 0.9	46.96 $\pm$ 14.6
<i>S. aureus</i>	10 mM $\beta$ -CD–AgNPs	99.06 $\pm$ 0.8	97.50 $\pm$ 0.8	98.14 $\pm$ 1.6	97.4 $\pm$ 0.8	93.97 $\pm$ 3.2	26.68 $\pm$ 10.5
<i>S. aureus</i>	5 mM $\beta$ -CD–AgNPs	98.62 $\pm$ 1.0	98.46 $\pm$ 1.5	97.04 $\pm$ 0.9	96.98 $\pm$ 0.9	66.58 $\pm$ 12.8	18.245 $\pm$ 6.3
<i>S. aureus</i>	Uncapped AgNPs	98.40 $\pm$ 0.8	97.31 $\pm$ 1.9	97.46 $\pm$ 1.0	96.88 $\pm$ 0.9	59.50 $\pm$ 7.6	16.97 $\pm$ 7.6

N/D, no growth inhibition detected.

<sup>a</sup> All values are the mean  $\pm$  standard deviation of two parallel experiments performed in triplicate.

3400  $\text{cm}^{-1}$ , indicating deprotonation of the hydroxyl groups [10] at the rim of the CD structure. This suggests that there is chemisorption between the CD molecules and AgNPs via the rim hydroxyl groups. Sorption of CDs might be due to binding of the AgNPs to hydroxyl groups at positions C<sub>2</sub> or C<sub>3</sub>. The oxyanion thus formed is less nucleophilic than the non-deprotonated hydroxyl at position C<sub>6</sub> [11] and is therefore more likely to bind to the AgNPs.

### 3.4. Particle sizing

TEM micrographs of capped and uncapped AgNPs showed them to be nearly spherical in shape, with the average size decreasing with increasing  $\beta$ -CD capping. DLS showed particles sizes of 6.2, 5.1 and 4.0 nm for  $\beta$ -CD-capped AgNPs (5, 10 and 20 mM, respectively) and 16.3 nm for the uncapped particle. The capped AgNPs were much larger in size than the  $\beta$ -CD cavity (0.78 nm), indicating chemisorption interaction through the CD rim hydroxyls rather than encapsulation.

### 3.5. Antibacterial activity

Most published AgNP antibacterial studies have used plate counting [12] and agar diffusion methods. Fewer reports have used the quantitative microtitre well dilution method. The effect of  $\beta$ -CD capping on antibacterial activity was determined by comparing the percentage inhibition of bacterial growth by uncapped AgNPs compared with that of capped AgNPs (5, 10 and 20 mM  $\beta$ -CD) using a range of Ag concentrations (100, 50, 25, 12.5, 6.25 and 3.12 ppm) detailed in Table 1.

$\beta$ -CD-capped AgNPs displayed significantly ( $P < 0.05$ ) greater antibacterial activity against *P. aeruginosa* than uncapped AgNPs. AgNPs capped with 20 mM and 10 mM  $\beta$ -CD had the strongest activity of 99.2% and 97.3% inhibition, respectively, at 12.5 ppm [Ag], whereas inhibition for AgNPs capped with 5 mM  $\beta$ -CD was 64.5% and for uncapped AgNPs was 13.9%. Both capped and uncapped AgNPs with a [Ag]  $\geq$  25 ppm significantly inhibited

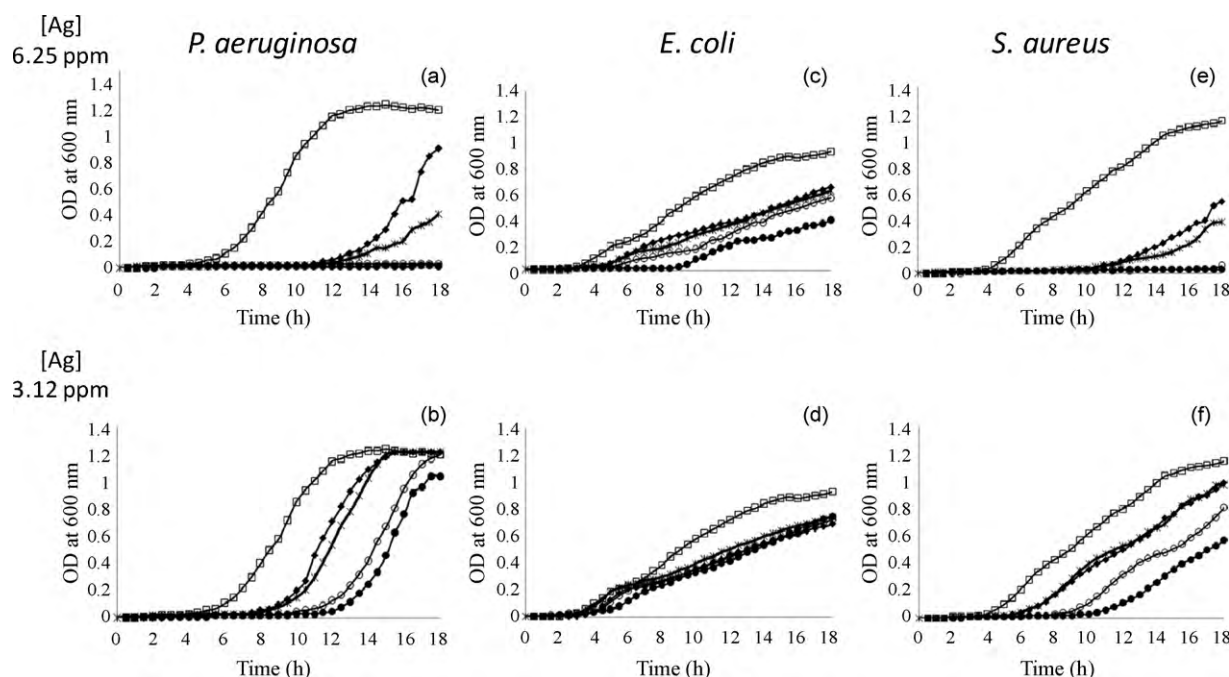


**Fig. 1.** Growth curves of (a, b) *Pseudomonas aeruginosa* in the presence of 6.25 ppm [Ag] (a) and 3.12 ppm [Ag] (b), (c, d) *Escherichia coli* in the presence of 6.25 ppm [Ag] (c) and 3.12 ppm [Ag] (d) and (e, f) *Staphylococcus aureus* in the presence of 6.25 ppm [Ag] (e) and 3.12 ppm [Ag] (f). (●) 20 mM  $\beta$ -cyclodextrin ( $\beta$ -CD); (○) 10 mM  $\beta$ -CD; (×) 5 mM  $\beta$ -CD; (◆) 0 mM  $\beta$ -CD; and (□) Ag/ $\beta$ -CD-free control. OD, optical density.

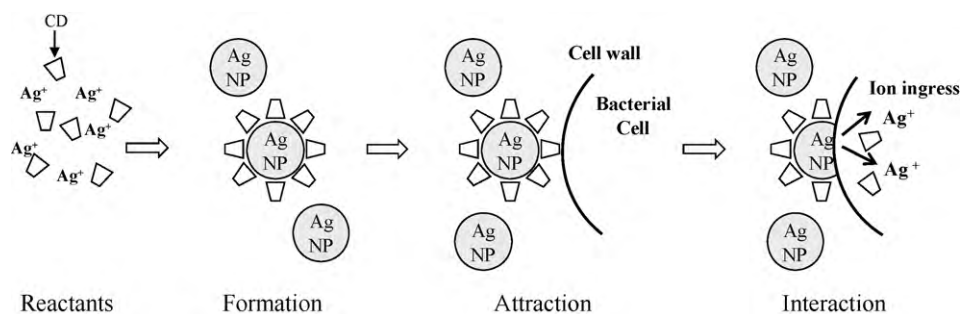


Fig. 2. Proposed bacterial interaction with  $\beta$ -cyclodextrin ( $\beta$ -CD)-capped silver nanoparticles (AgNPs).

bacterial growth, whilst those with a  $[Ag] \leq 6.25$  ppm showed no inhibition.

*Escherichia coli* was 97% inhibited at a  $[Ag]$  of  $\geq 12.5$  ppm. Below this there was a variation in inhibition, with 20 mM  $\beta$ -CD-capped AgNPs achieving 53.5% inhibition at 6.25 ppm, whereas uncapped AgNPs showed only 22.8% inhibition.

*Staphylococcus aureus* was 97.1% inhibited by 20 mM  $\beta$ -CD-capped AgNPs at a  $[Ag]$  of 6.25 ppm compared with 59.5% inhibition by uncapped AgNPs. Antibacterial activity was high (94.0% inhibition) even at a concentration of 10 mM  $\beta$ -CD. Similar findings were obtained with a  $[Ag]$  of 3.12 ppm.

Antibacterial activity increased with corresponding rises in both silver and cyclodextrin concentrations in all cases. Importantly,  $\beta$ -CD alone showed no antibacterial activity.

Bacterial growth curves showed that the AgNPs delayed growth. The 20 mM and 10 mM  $\beta$ -CD-capped AgNPs containing a  $[Ag]$  of 6.25 ppm completely inhibited *P. aeruginosa* growth until 18 h (Fig. 1a) compared with ca. 10 h for the uncapped AgNPs. Even at a  $[Ag]$  of 3.12 ppm the 20 mM  $\beta$ -CD-capped AgNPs were more effective than uncapped AgNPs (Fig. 1b). The 20 mM  $\beta$ -CD-capped AgNPs at a  $[Ag]$  of 6.25 ppm exhibited superior antibacterial activity against *E. coli* compared with uncapped AgNPs, delaying growth for 9 h versus 4.5 h (Fig. 1c). A similar trend was observed for the 10 mM and 5 mM  $\beta$ -CD-capped AgNPs. At a  $[Ag]$  of 6.25 ppm, AgNPs capped with 20 mM and 10 mM  $\beta$ -CD delayed growth of *S. aureus* for 17 h (Fig. 1e). At a  $[Ag]$  of 3.12 ppm capping doubled growth inhibition (Fig. 1f). Overall, the duration of the lag growth phase of the test organisms when grown in the presence of AgNPs with different  $[Ag]$  increased as the  $\beta$ -CD capping concentration increased.

The increased antibacterial activity of  $\beta$ -CD-capped AgNPs may be attributed to a biodegradable capping agent forming smaller nanoparticles without aggregation. These have a high surface-to-volume ratio and undergo a higher level of interaction with the bacterial cell surface than the larger uncapped AgNPs, resulting in a higher antibacterial activity.

It is proposed that intimate contact between AgNPs and organisms may enhance the transfer of Ag ions to the bacterial cell, whilst bacterial degradation of the  $\beta$ -CD saccharide promotes the release of silver ions (Fig. 2) [13]. Such interactions have been described as Trojan-horse mechanisms and have been reported in the literature where fetal bovine serum was used to improve AgNP efficacy [14]. These results are in accordance with a previous report in which AgNPs synthesised by disaccharides had higher antibacterial activities than those synthesised by monosaccharides [15].

#### 4. Conclusion

In summary, there was an increase in the antibacterial activity of  $\beta$ -CD-capped AgNPs compared with their uncapped equivalents. This activity increased as the concentration of  $\beta$ -CD increased. Thus,  $\beta$ -CD capping can be used to achieve higher antibacterial efficacies at lower metal ion concentrations.

**Funding:** The authors wish to acknowledge the Dublin Institute of Technology (Dublin, Ireland) for funding under the ABBEST scholarship programme (SJ) and Enterprise Ireland under the ARE Programme (BD and NS).

**Competing interests:** None declared.

**Ethical approval:** Ethical approval was received from the Dublin Institute of Technology (DIT) Ethics Committee (Internal DIT code Ref 52/09).

#### Acknowledgements

The authors wish to thank Ted Doody for assistance with antimicrobial assays.

#### References

- [1] Sharma KV, Yngard AR, Lin Y. Silver nanoparticles: green synthesis and their antimicrobial activities. *Adv Colloid Interface Sci* 2009;145:83–96.
- [2] Feng QL, Wu J, Chen GQ, Cui FZ, Kim TN, Kim JO. A mechanistic study of the antibacterial effect of silver ions on *Escherichia coli* and *Staphylococcus aureus*. *J Biomed Mater Res* 2000;52:662–8.
- [3] Stobie N, Duffy B, McCormack DE, Colreavy J, Hidalgo M, McHale P, et al. Prevention of *Staphylococcus epidermidis* biofilm formation using a low-temperature processed silver-doped phenyltriethoxysilane sol-gel coating. *Biomaterials* 2008;29:963–9.
- [4] Sing S, Patel P, Jaiswal S, Prabhune AA, Ramana CV, Prasad BLV. A direct method for the preparation of glycolipid-metal nanoparticle conjugates: sophorolipids as reducing and capping agents for the synthesis of water re-dispersible silver nanoparticles and their antibacterial activity. *New J Chem* 2009;33:646–52.
- [5] Rekharsky MV, Inoue Y. Complexation thermodynamics of cyclodextrins. *Chem Rev* 1998;98:1875–918.
- [6] Donova MV, Nikolayeva VN, Dovbnya DV, Gulevskaya SA, Suzina NE. Methyl- $\beta$ -cyclodextrin alters growth, activity and cell envelope features of sterol-transforming mycobacteria. *Microbiology* 2007;153:1981–92.
- [7] Casey JT, O'Cleirigh C, Walsh PK, O'Shea DG. Development of a robust microtiter plate-based assay method for assessment of bioactivity. *J Microbiol Methods* 2004;58:327–34.
- [8] Slistan-Grijalva A, Herrera-Urbina R, Rivas-Silva JF, Avalor-Borja M, Castellón-Barraza FF, Posada-Amarillas A. Classical theoretical characterization of the surface plasmon absorption band for silver spherical nanoparticles suspended in water and ethylene glycol. *Physica E Low Dimens Syst Nanostruct* 2005;27:104–12.
- [9] Egyed O. Spectroscopic studies on  $\beta$ -cyclodextrin. *Vib Spectrosc* 1990;1:225–7.
- [10] Cortés ME, Sinisterra RD, Campos MJA, Tortamano N, Rocha RG. The chlorhexidine- $\beta$ -cyclodextrin inclusion compound: preparation, characterization and microbiological evaluation. *J Incl Phenom Macrocyclic Chem* 2001;40:297–302.
- [11] Cruz LAC, Perez CAM, Romero HAM, Casillas PEG. Synthesis of magnetite nanoparticles- $\beta$ -cyclodextrin complex. *J Alloys Compd* 2008;466:330–4.
- [12] Pal S, Tak YK, Song JM. Does the antibacterial activity of silver nanoparticles depend on the shape of the nanoparticle? A study of the Gram-negative bacterium *Escherichia coli*. *Appl Environ Microbiol* 2007;73:1712–20.
- [13] Loher S, Schneider OD, Maienfisch T, Bokorny S, Stark WJ. Micro-organism-triggered release of silver nanoparticles from biodegradable oxide carriers allows preparation of self-sterilizing polymer surfaces. *Small* 2008;4:824–32.
- [14] Park EJ, Yi J, Kim Y, Choi K, Park K. Silver nanoparticles induce cytotoxicity by a Trojan-horse type mechanism. *Toxicol In Vitro* 2010;24:872–8.
- [15] Panáček A, Kvítek L, Prucek R, Kolář M, Večeřová R, Pizárová N, et al. Silver colloid nanoparticles: synthesis, characterization, and their antibacterial activity. *J Phys Chem B* 2006;10:16248–53.